



# OPEN White matter volume and microstructural integrity are associated with fatigue in relapsing multiple sclerosis

Alejandra Figueroa-Vargas<sup>1,2,12</sup>✉, Sebastián Navarrete-Caro<sup>3,12</sup>, Claudia Cárcamo<sup>4</sup>, Ethel Ciampi<sup>4,5</sup>, Macarena Vásquez-Torres<sup>4</sup>, Bernardita Soler<sup>4,5</sup>, Cristian Montalba<sup>4</sup>, Matías Iriarte-Carter<sup>1</sup>, María Paz Martínez-Molina<sup>1,6</sup>, Patricio Carvajal-Paredes<sup>1</sup>, Mariana Ayala-Ochoa<sup>1</sup>, Víctor Márquez-Rodríguez<sup>1</sup>, Paulo Figueroa-Taiba<sup>1</sup>, Marcela Díaz-Díaz<sup>1,7</sup>, Joaquín Herrero<sup>2,8</sup>, Rodrigo Henríquez-Ch<sup>2</sup>, Ximena Stecher<sup>9</sup>, Carla Manterola<sup>10</sup>, Francisco Zamorano<sup>9,11</sup>, Pamela Guevara<sup>3</sup>, Francisco Aboitiz<sup>2</sup>✉ & Pablo Billeke<sup>1</sup>✉

Multiple sclerosis (MS) is a prevalent neurological disorder marked by inflammation and demyelination, with fatigue being one of the most reported and debilitating symptoms. While fatigue occurs across various neurological conditions and even in healthy individuals, the specific mechanisms contributing to fatigue in each context remain unclear. In this study, we conducted a cross-sectional analysis involving 32 people with relapsing MS (PwRMS) and 29 healthy controls who reported fatigue. Participants underwent MRI scans, including T1-weighted and diffusion-weighted imaging. Additionally, the Modified Fatigue Impact Scale was utilized. We employed Bayesian LASSO and Spike-and-Slab LASSO regression models to investigate the hypothesis that fatigue correlates differently with brain structures in PwRMS. Our findings revealed brain regions associated with general and cognitive fatigue. In particular, reduced white matter volume and compromised microstructural integrity in specific areas—such as the cingulate gyrus, inferior frontal gyrus, and the banks of the superior temporal sulcus—showed significant associations with fatigue scores in PwRMS. These results suggest that alterations in specific brain regions may play a critical role in the clinical manifestation of fatigue in MS. Understanding these insights could help differentiate general mechanisms of fatigue from those affecting people with relapsing MS, which may guide future therapeutic strategies.

**Keywords** People with relapsing multiple sclerosis (PwRMS), Fatigue, Inferior frontal gyrus (IFG), Frontal pole, Magnetic resonance imaging (MRI), Diffusion tensor imaging (DTI)

Multiple sclerosis is the most common neurological non-traumatic condition that generates disability in young adults<sup>1,2</sup>. Relapsing multiple sclerosis (RMS) represents the most prevalent subtype of MS, accounting for

<sup>1</sup>Laboratorio de Neurociencia Social y Neuromodulación (NeuroCICS), Centro de Investigación en Complejidad Social, Facultad de Gobierno, Universidad del Desarrollo, Las Condes, Chile. <sup>2</sup>Laboratorio LaNCE, Centro Interdisciplinario de Neurociencia, Facultad de Medicina, Pontificia Universidad Católica de Chile, Santiago, Chile. <sup>3</sup>Departamento de Ingeniería Eléctrica, Facultad de Ingeniería, Universidad de Concepción, Concepción, Chile. <sup>4</sup>Programa de Esclerosis Múltiple, Facultad de Medicina, Pontificia Universidad Católica de Chile, Santiago, Chile. <sup>5</sup>Unidad de Neuroinmunología, Servicio de Neurología, Complejo Asistencial Doctor Sótero del Río, Puente Alto, Chile. <sup>6</sup>Centro de Investigación y Desarrollo en Ciencias Aeroespaciales (CIDCA), Academia Politécnica Aeronáutica (APA) Fuerza Aérea de Chile, El Bosque, Chile. <sup>7</sup>Facultad de Psicología, Universidad San Sebastián, Santiago, Chile. <sup>8</sup>Facultad de Medicina, Escuela de Kinesiología, Finis Terrae University, Providencia, Chile. <sup>9</sup>Unidad de Imágenes Cuantitativas Avanzadas, Departamento de Imágenes, Facultad de Medicina, Clínica Alemana-Universidad del Desarrollo, Las Condes, Chile. <sup>10</sup>Departamento de Pediatría, Facultad de Medicina, Clínica Alemana-Universidad del Desarrollo, Las Condes, Chile. <sup>11</sup>Facultad de Ciencias para el Cuidado de la Salud, Universidad San Sebastián, Santiago, Chile. <sup>12</sup>Alejandra Figueroa-Vargas and Sebastián Navarrete have contributed equally to this work. ✉email: amfigueroa@udd.cl; faboitiz@uc.cl; pbilleke@udd.cl

approximately 85% of cases at diagnosis. It is characterized by episodes of neurological dysfunction or relapses, followed by periods of remission, during which there is either partial or full recovery<sup>3</sup>. Fatigue is one of the most frequently reported and disabling symptoms in people with multiple sclerosis (PwMS), affecting an estimated 60–80% of this population<sup>4,5</sup>. Fatigue negatively impacts the quality of life, employment, psychological state, and daily functioning<sup>6,7</sup>. Fatigue is difficult to define and measure objectively, especially in PwMS. Currently, most fatigue assessments for PwMS rely on self-reported measures, with several widely recognized instruments available, including the Modified Fatigue Impact Scale (MFIS)<sup>8,9</sup>.

The pathophysiological mechanisms underlying fatigue may involve central factors, such as disruptions in neuronal energetics, function, or signal conduction<sup>10</sup>; peripheral mechanisms, including muscular dysfunction<sup>11</sup>; or systemic factors, such as immune system dysregulation<sup>12</sup>. Despite significant efforts to understand the mechanisms underlying fatigue, these have not yet been elucidated<sup>4,13,14</sup>. Beyond PwMS, fatigue is a symptom observed in various medical conditions, with its prevalence significantly increasing in diseases involving immune system dysregulation. These include cancer, chronic infections, autoimmune diseases, and neurological disorders such as rheumatoid arthritis<sup>15</sup>, lupus<sup>16</sup>, Long COVID<sup>17</sup>, and cancer<sup>18</sup>.

Fatigue has also been reported even in healthy individuals, with a general prevalence of 20.4% among healthy adults<sup>19</sup>. Moderate fatigue occurs 2.4 times more frequently than severe fatigue. Interestingly, unexplained fatigue—defined as fatigue without a clear medical cause—is approximately 2.7 times more prevalent than fatigue attributable to underlying medical conditions<sup>19</sup>. In clinical practice, fatigue ranks among the top five most commonly presented complaints in primary care settings<sup>20</sup>, reflecting its widespread impact. These findings indicate that fatigue can manifest in healthy individuals without identifiable medical or psychological conditions. Fatigue has been hypothesized to function as an adaptive mechanism, evolved to protect the body from potential harm under various conditions, even in the absence of overt pathology<sup>21</sup>. However, unexplained fatigue in healthy individuals has been associated with long-term risks of developing metabolic, immunological, or psychiatric dysfunctions<sup>22</sup>. Notably, approximately half of those initially presenting with fatigue eventually receive a diagnosis of a medical condition, including infections, anemia, thyroid dysfunction, diabetes mellitus, or cancer<sup>22</sup>. Additional contributing factors include sleep disorders, sleep-related breathing disorders, excessive psychosocial stress<sup>23</sup>, lifestyle-related exposures (e.g., smoking, alcohol consumption)<sup>24</sup>, and post-COVID-19 effects<sup>25</sup>. These observations underscore the complexity of fatigue as a symptom, suggesting that its underlying pathophysiological mechanisms are multifactorial. These features complicate the distinction between general fatigue and pathology-specific or patient-specific causes<sup>26</sup>, ultimately limiting the effectiveness of therapeutic strategies tailored to resolve each patient's condition.

MRI is a widely utilized non-invasive imaging technique in clinical practice that enables the *in vivo* detection of central nervous system (CNS) damage associated with MS<sup>27–29</sup>. Structural MRI has been extensively employed to investigate brain abnormalities in PwMS, offering valuable insights into the location and severity of structural damage, including gray matter, white matter lesion (WML) burden, and brain atrophy<sup>29,30</sup>. Although conventional MRI provides valuable insights through qualitative evaluations or volumetric analyses, relying solely on these techniques to explain clinical symptomatology in MS is limited and often inconsistent<sup>4</sup>. Incorporating quantitative analyses and advanced imaging methods like quantitative MRI measures and diffusion MRI (dMRI) is crucial<sup>31</sup> to overcome these limitations. dMRI enables the exploration of subtle brain abnormalities by assessing structural connectivity, revealing how different brain regions are interconnected to form networks<sup>32</sup>. In MS, microstructural damage to tissues, including myelin and axons, is a defining feature, even in the early stages of the disease<sup>3</sup>. Such damage disrupts structural connectivity, impairing functional connectivity<sup>33,34</sup>. These disruptions in brain networks likely play a pivotal role in the clinical manifestation of MS symptoms<sup>35</sup>, including fatigue<sup>36,37</sup>.

Previous studies have identified abnormalities in the cortico-striato-thalamo-cortical loop as key contributors to fatigue in various subtypes of MS<sup>38–40</sup>. However, brain connectivity changes specific to fatigue in PwMS have yet to be thoroughly investigated<sup>3</sup>. Given that the pathophysiological mechanisms and clinical characteristics of relapsing MS differ significantly from those of progressive MS subtypes<sup>41</sup>, examining the underlying brain alterations associated with fatigue is crucial, specifically within this group. In this study, we aimed to assess the relationship between brain structural MRI measures, including volume and connectivity and reported fatigue in PwMS and control participants with subjective fatigue but no neurological conditions. This approach may offer new insights into distinguishing general mechanisms underlying fatigue from those specifically impacting PwMS.

## Results

### Descriptive of the participant characteristics

The characteristics of the PwMS and HC experiencing fatigue are shown in Table 1. For PwMS, the median age of 32 participants was 36.67 years (IQR = 10.76); 59.3% were female, and schooling was 18 years (IQR = 2). The median of disease duration was 7 years (IQR = 5.25). Disease-modifying therapies (DMT) included 4 PwMS in the low efficacy (12.5%), 7 in the moderate efficacy (21.9%), and 21 in the high efficacy (65.6%)<sup>42</sup>. The median total MFIS score was 41.50 (IQR = 20.5); the median cognitive subitem MFIS score was 20 (IQR = 10.5); the median physical subitem MFIS score was 19 (IQR = 10.25), and the median psychosocial subitem MFIS score was 3 (IQR = 3). Four PwMS had depression diagnoses under treatment. The median Z score for Paced Auditory Serial Addition (zPASAT) was 0.45 (IQR = 0.95), and the median Z score for the Symbol Digit Modalities Test (zSDMT) was 0.5 (IQR = 0.87). The median of the Generalized Anxiety Disorder 7-item (GAD-7) was 4 (IQR = 4), and the median of the Spanish version of the Patient Health Questionnaire-9 (PHQ-9) was 4 (IQR = 3.5). For healthy controls experiencing fatigue, the median age of 29 participants was 39.18 years (IQR = 10.39) (no differences between groups,  $t(59) = -0.72$ ,  $p = 0.46$ ); 58.6% were female (no differences between groups,  $\chi^2 = 0$ ,  $df = 1$ ,  $p = 1$ ), and schooling was 18 years (IQR = 2) (no differences between groups,  $t(59) = -0.55$ ,

	PwRMS	Healthy Controls	<i>p</i> -value*
	( <i>n</i> = 32)	( <i>n</i> = 29)	
Age, years, median (IQR)	36.67 (10.76)	39.18 (10.39)	0.46
Sex, <i>n</i> (%)			0.2
Female	19 (59.3)	17 (58.6)	
Male	13 (40.7)	12(41.4)	
Schooling, years, median (IQR)	18(2)	18(2)	0.58
Disease duration, years, median (IQR)	7 (5.25)		-
Race, <i>n</i> (%)			
White	32 (100%)	29 (100%)	-
Hispanic, Latino ethnicity, <i>n</i> (%)			
Yes	32 (100%)	29 (100%)	-
DMT, <i>n</i> (%)			
Low	4 (12.5)		-
Moderate	7 (21.9)		-
High	21 (65.6)		-
MFIS, median (IQR)			
Total	41.50 (20.5)	42 (17)	0.47
Cognitive	20 (10.5)	20 (8)	0.67
Physical	19 (10.25)	18 (7)	0.32
Phycosocial	3 (3)	3 (2)	0.89
Depression, <i>n</i> (%)			1
No	28	26	
Yes	4	3	
Unknown	0	0	
EDSS, median (IQR)	1 (1)		-
zPASAT, median (IQR)	0.45 (0.95)		-
zSDMT, median (IQR)	0.5 (0.87)	0 (0.8)	0.03
GAD-7, median (IQR)	4 (4)	3 (4)	0.7
PHQ-9, median (IQR)	4 (3.5)	4 (4)	0.8

**Table 1.** Comparison of characteristics between PwRMS and healthy controls. **IQR:** Interquartile Range; **DMT:** disease-modifying therapies; **MFIS:** Modified Fatigue Impact Scale; **EDSS:** Expanded Disability Status Scale; **zPASAT:** Z score Paced Auditory Serial Addition Test; **zSDMT:** Z score Symbol Digit Modalities Test; **GAD-7:** Generalized Anxiety Disorder 7-item; **PHQ-9:** Patient Health Questionnaire 9-item.

$p = 0.58$ ). The median total MFIS score was 42 (IQR = 17) (no differences between groups,  $t(59) = 0.72$ ,  $p = 0.47$ ); the median cognitive subitem MFIS score was 20 (IQR = 8) (no differences between groups,  $t(59) = 0.42$ ,  $p = 0.67$ ); the median physical subitem MFIS score was 18 (IQR = 7) (no differences between groups,  $t(59) = 0.99$ ,  $p = 0.32$ ), and the median psychosocial subitem MFIS score was 3 (IQR = 2) (no differences between groups,  $t(59) = 0.12$ ,  $p = 0.89$ ). The median zSDMT was 0.09 (IQR = 0.8) (with a significantly smaller difference compared to PwRMS,  $t(59) = 2.05$ ,  $p = 0.044$ ). Three fatigued healthy controls had depression diagnoses under treatment (no differences between groups,  $\chi^2 = 1e-31$ ,  $df = 1$ ,  $p = 1$ ). The median of GAD-7 was 3 (IQR = 4), (no differences between groups,  $t(59) = 0.3$ ,  $p = 0.7$ ), and the median of the Spanish version of the PHQ-9 was 4 (IQR = 4), (no differences between groups,  $t(59) = 0.19$ ,  $p = 0.8$ ).

**Association between structural MRI measures and total fatigue score**

First, we calculated the volumes of cortical and subcortical gray matter and white matter for PwRMS and HC experiencing fatigue using the first two steps of the Human Connectome Project (HCP) pipeline (see Methods). Second, we calculated the Principal Components Analysis (PCA) for each group's cortical and subcortical gray matter and white matter and selected the first twenty Principal Components (PC) that had a main contribution. Third, we implemented Bayesian Least Absolute Shrinkage and Selection Operator (LASSO) and Bayesian Spike-and-Slab LASSO (SSL) linear regression models to examine relationships between compositional predictors—including the PCA of cortical, subcortical gray matter, and white matter volumes—and total fatigue scores. This analysis detected relationships and differences within and between groups (PwRMS and healthy individuals experiencing fatigue) in volumetric associations with self-reported fatigue scores (see Methods and Eq. 1 for further details). Using this approach, we evaluated the components that accounted for the highest percentage of participant variance, minimizing the risk of false positive results (see Methods for further details). Specifically, using PCA with LASSO allows for dimensionality reduction and effective control of multicollinearity, enhancing model robustness and interpretability while minimizing the risk of overfitting<sup>43</sup>.

For the regressions involving subcortical and cortical gray matter, none of the components showed a significant relationship with fatigue in either MS patients or HC individuals experiencing fatigue. For the regression of white matter, we found that one of the components selected in the PCA analysis, specifically PC #15 of the white matter volumes, showed a significant relationship with fatigue in PwRMS (LASSO: posterior distribution mean: 11.5, 95%HDI [2.4 21.2],  $p_{\text{MCMC}}=0.01$ ; SSL mean: 8.5, 95%HDI [0.01 17.7],  $p_{\text{MCMC}}=0.04$ ), lead a significant difference in its relation between the PwRMS and fatigued healthy controls (LASSO: posterior distribution mean: 7.7, 95%HDI [1.6 13.6],  $p_{\text{MCMC}}=0.0072$ ; SSL means 5.8, 95%HDI = [0.01 11.5],  $p_{\text{MCMC}}=0.03$ , Fig. 1). These differences persist even after controlling for depressive and anxiety symptoms using the GAD-7 and PHQ-9 scales (PwRMS posterior distribution mean: 4.15, 95% HDI [0.1, 8.21],  $p_{\text{MCMC}} = 0.04$ ; PwRMS > HC posterior distribution mean: 7.75, 95% HDI [1.84, 13.51],  $p_{\text{MCMC}} = 0.0064$ ).

Next, we identified the brain regions that constitute this component. Specifically, the top twenty white matter regions contributing to PC #15, ranked by their absolute loading values from highest to lowest, are presented in Table 2 and illustrated in Fig. 1. These first twenty principal white matter regions included were the left hemisphere caudal anterior cingulate, left hemisphere pars triangularis of the inferior frontal gyrus, right hemisphere banks of the superior temporal sulcus, left hemisphere transverse temporal region, right hemisphere insula, left hemisphere cerebellum, left hemisphere entorhinal region, right hemisphere lateral occipital region, right hemisphere rostral anterior cingulate gyrus, and left hemisphere paracentral gyrus.

### Association between MRI connectivity measures and total fatigue score

Regarding the analysis of FA, we calculated this measure in all the fiber bundles that connected the areas of PC15, and that could be determined in all participants. Thus, four bundles were tested using LASSO and SSL models. A significant increase in FA was found for the Superficial White Matter (SWM) fibers that connect

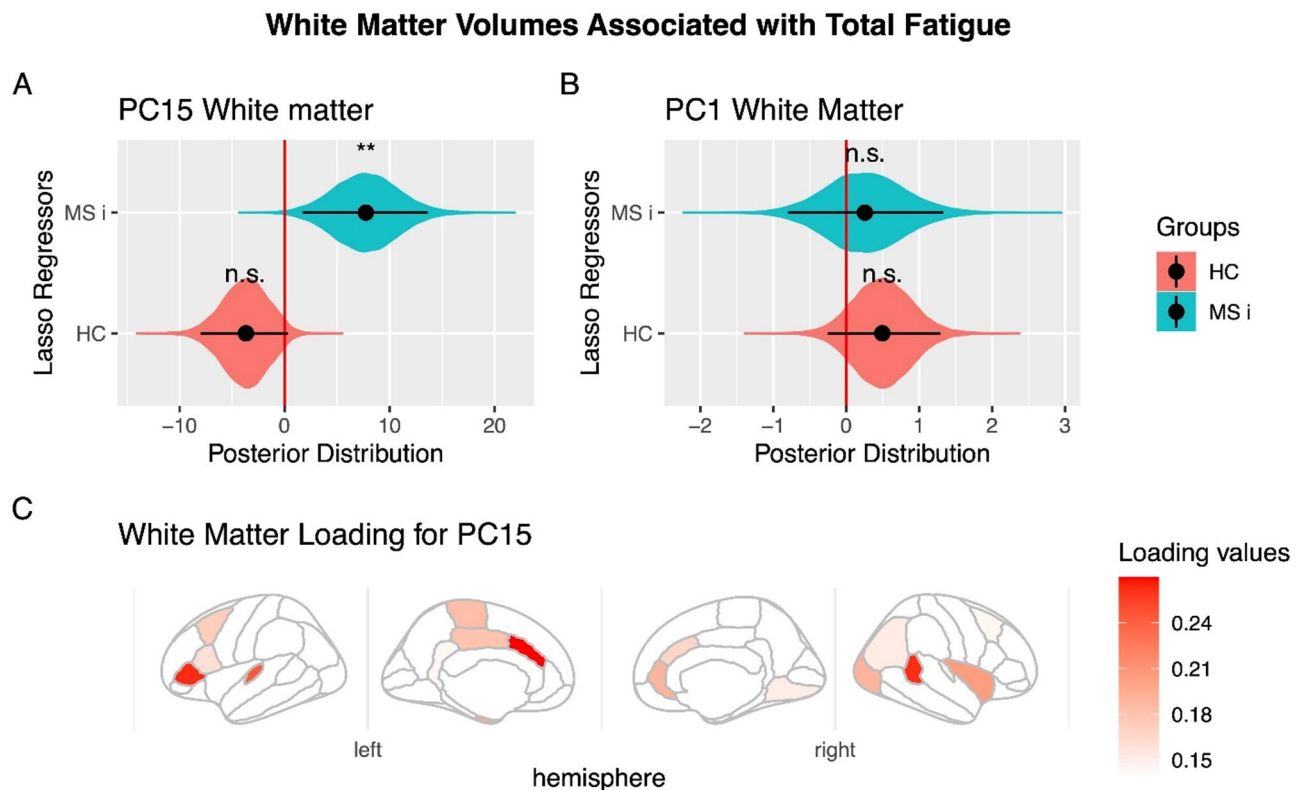


**Fig. 1.** White Matter Volumes Associated with Total Fatigue. **(A)** Principal Component #15 (PC15) demonstrated significant modulation in people with relapsing multiple sclerosis (PwRMS). They showed a significant interaction between PwRMS and healthy controls experiencing fatigue (HC). **(B)** Principal Component #1 (PC1) showed no significant association with fatigue measures. **A–B:** The black dot indicates the median, the line shows the 95% high-density interval of the posterior distribution, and the shaded area represents the entire posterior distribution. **(C)** Loading for PC15. The main white matter volumes are shown according to absolute values of loading of PC15. In the *right hemisphere*: banks of the superior temporal sulcus (0.26), insula (0.20), lateral occipital (0.19), rostral anterior cingulate (0.19). In the *left hemisphere*: caudal anterior cingulate (0.27), pars triangularis (0.26), transverse temporal (0.24), cerebellum (0.20) (it is not visible in the figure), cortex entorhinal (0.20), and paracentral (0.18). HC: Healthy control experience fatigue, MC i: Multiple sclerosis interaction, that means the difference in the correlation between HC and patients with multiple sclerosis, *rh*: right hemisphere, *lh*: left hemisphere. Statistical significance levels: n.s., no significant difference; \* $p < 0.05$ ; \*\* $p < 0.01$ ; \*\*\* $p < 0.001$ .

Principal Component #8		Principal Component #13		Principal Component #15	
White Matter Region	Loading (Absolute Value)	White Matter Region	Loading (Absolute Value)	White Matter Region	Loading (Absolute Value)
lh lateral occipital	2.9	lh banks sts	3.1	lh caudal anterior cingulate	2.7
rh frontal pole	2.6	rh banks sts	3.1	lh pars triangularis (ifg)	2.6
lh entorhinal	2.4	lh pars orbitalis (ifg)	2.8	rh banks sts	2.6
lh rostral anterior cingulate	2.2	lh isthmus cingulate	2.8	lh transverse temporal	2.4
rh caudal middle frontal	2.1	rh frontal pole	2.3	rh insula	2.0
optic chiasm	2.1	rh parahippocampal	2.2	lh cerebellum	2.0
lh supramarginal	2.0	rh temporal pole	2.2	lh entorhinal	2.0
lh parahippocampal	1.8	rh pars triangularis (ifg)	2.1	rh lateral occipital	1.9
rh insula	1.7	corpus callosum (anterior)	2.0	rh rostral anterior cingulate	1.9
lh transverse temporal	1.6	rh entorhinal	2.0	lh paracentral	1.8
lh posterior cingulate	1.6	rh isthmus cingulate	1.9	lh posterior cingulate	1.8
lh pars orbitalis (ifg)	1.6	lh entorhinal	1.9	lh caudal middle frontal	1.7
lh middle temporal	1.5	rh transverse temporal	1.6	rh caudal anterior cingulate	1.7
rh pars triangularis (ifg)	1.5	lh temporal pole	1.6	lh pars opercularis (ifg)	1.6
lh caudal anterior cingulate	1.4	optic chiasm	1.4	rh inferior parietal	1.5
rh entorhinal	1.4	rh pars orbitalis (ifg)	1.4	rh lingual	1.5
lh precuneus	1.4	lh inferior parietal	1.4	rh transverse temporal	1.5
rh transverse temporal	1.4	lh posterior cingulate	1.3	lh isthmus cingulate	1.4
lh pars triangularis (ifg)	1.4	lh rostral anterior cingulate	1.2	rh caudal middle frontal	1.4
corpus callosum (central)	1.4	lh rostral middle frontal	1.0	rh parahippocampal	1.4

**Table 2.** White matter region and loading in key PC. rh: right hemisphere, lh: left hemisphere, sts: superior temporal sulcus, ifg: inferior frontal gyrus.

within the region Pars Triangularis (LASSO posterior distribution mean = 86.2, 95%HDI = [29 143],  $p_{\text{MCMC}}=0.0019$ ; SSL mean = 98.3, 95%HDI = [48 146],  $p_{\text{MCMC}}=0.0001$ ; Fig. 2).

### Association between white matter volume and cognitive fatigue

Finally, to gain deeper insight into specific aspects of fatigue related to changes in white matter volume, we conducted additional analyses. First, we applied the same approaches using LASSO and SSL on principal components in separate regression models for cognitive and physical fatigue. Notably, for cognitive fatigue, principal component #15 consistently correlated with symptoms in PwRMS patients but not in HC experiencing fatigue (LASSO: posterior distribution mean: 2.6, 95%HDI [0.8 4.5],  $p_{\text{MCMC}}=0.008$ ; SSL mean: 1.9, 95%HDI [0.07 4.0],  $p_{\text{MCMC}}=0.03$ ), lead a significant difference in its relation between the PwRMS and HC experiencing fatigue (LASSO: posterior distribution mean: 4.4, 95%HDI [1.6 13.6],  $p_{\text{MCMC}}=0.001$ ; SSL means 3.3, 95%HDI = [0.5 6.2],  $p_{\text{MCMC}}=0.01$ ). No significant regressors were identified for physical fatigue.

The preceding findings could be interpreted as suggesting that white matter is more closely related to cognitive fatigue than to physical fatigue. However, it is essential to note the high correlation between these two scores (Spearman's Rho = 0.65,  $p = 1e-8$ ,  $n = 61$ ). To further clarify this relationship, we conducted an additional regression analysis that included physical fatigue as a regressor for cognitive fatigue, aiming to isolate the brain-related deficits specific to the cognitive component. Again, the component 15 were found significant (LASSO: posterior distribution mean: 1.8, 95%HDI [0.6 3.2],  $p_{\text{MCMC}}=0.005$ ; SSL mean: 1.6, 95%HDI [0.01 3.5],  $p_{\text{MCMC}}=0.03$ ; difference between MS patients and HC: LASSO: posterior distribution mean: 2.3, 95%HDI [0.4 4.2],  $p_{\text{MCMC}}=0.01$ ; SSL mean: 1.2, 95%HDI [0.01 2.7],  $p_{\text{MCMC}}=0.04$ ). Moreover, this analysis revealed two additional components—PC #8 and PC #13—that are related to cognitive fatigue (PC #8 LASSO: posterior distribution mean: 1.9, 95%HDI [0.89 3.0],  $p_{\text{MCMC}}=0.0006$ ; SSL mean: 1.4, 95%HDI [0.2 2.6],  $p_{\text{MCMC}}=0.04$ ; difference between MS patients and HC: LASSO: posterior distribution mean: 2.3, 95%HDI [0.9 3.7],  $p_{\text{MCMC}}=0.001$ ; SSL mean: 1.5, 95%HDI [0.07 3.0],  $p_{\text{MCMC}}=0.03$ ; PC #13 LASSO: posterior distribution mean: 2.0, 95%HDI [0.6 3.3],  $p_{\text{MCMC}}=0.002$ ; SSL mean: 1.4, 95%HDI [0.01 2.9],  $p_{\text{MCMC}}=0.03$ ; difference between MS patients and HC: LASSO: posterior distribution mean: 2.8, 95%HDI [1.0 4.6],  $p_{\text{MCMC}}=0.001$ ; SSL mean: 1.7, 95%HDI [0.02 3.6],  $p_{\text{MCMC}}=0.04$ ). These two components share key regions identified in the preceding analysis, including the cingulate cortex, the banks of the superior temporal sulcus, and the inferior frontal gyrus, among others (see Fig. 3 for further details).

### Discussion

This study provides novel insights into the relationship between structural abnormalities and connectivity changes associated with fatigue in PwRMS compared to HC experiencing fatigue. Our findings reveal distinct white matter volumetric patterns and structural connectivity contributing to fatigue, particularly in goal-directed decision-making, language, sensorial integration, emotional, and social processing regions.

Our study's most significant findings include identifying specific white matter volumes that correlate differently with total fatigue, as evaluated by the MFIS, between PwRMS and HC experiencing fatigue. Regarding



## MRI connectivity measures and total fatigue score.

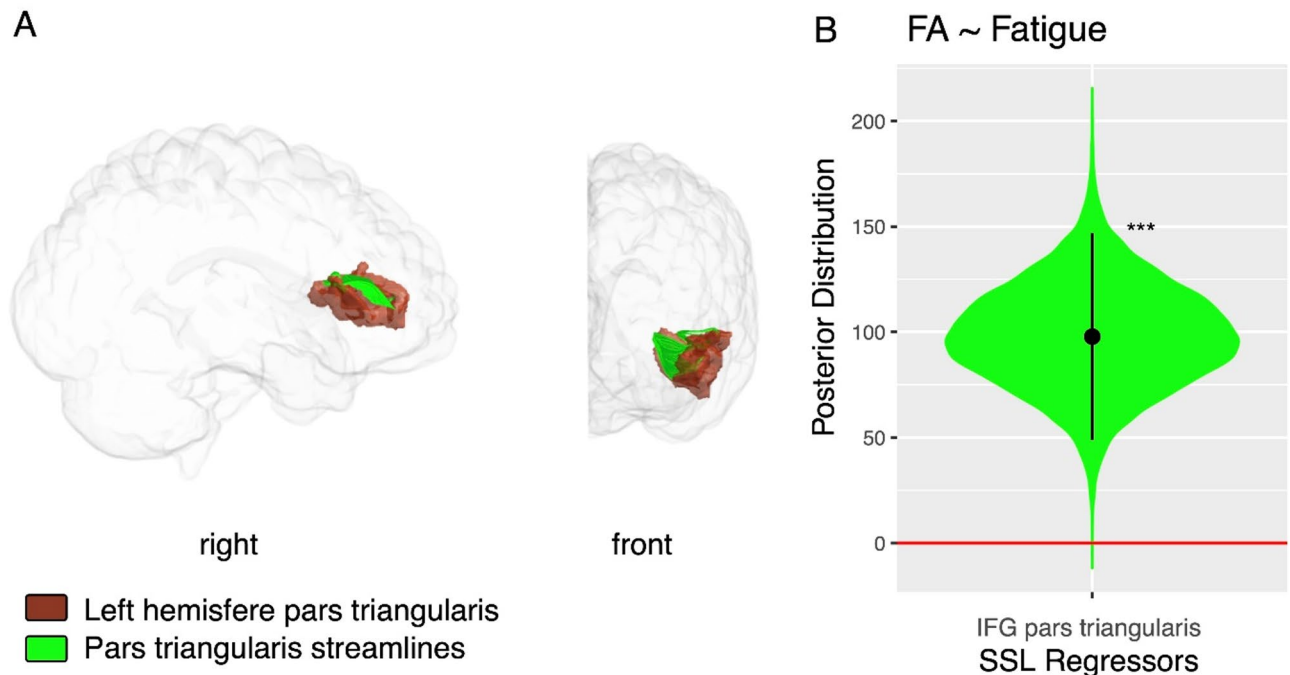


**Fig. 2.** MRI connectivity measures and total fatigue score. **(A)** Visualization of white matter volumes in the left hemisphere's Inferior Frontal Gyrus (Pars Triangularis) is shown in brown, with connecting fibers highlighted in green in patients with multiple sclerosis. **(B)** Posterior distribution of the regressor for Fractional Anisotropy in SWM fibers connecting regions within the Inferior Frontal Gyrus (Pars Triangularis) for the fatigue SSL model. IFG, Inferior Frontal Gyrus; FA, Fractional Anisotropy. Statistical significance levels: n.s., no significant difference; \* $p < 0.05$ ; \*\* $p < 0.01$ ; \*\*\* $p < 0.001$ .

the fatigue subitems, we found a significant relationship with white matter volumes only for cognitive fatigue exclusively in PwRMS, with a notable interaction between PwRMS and HC experiencing fatigue. However, no significant effects were found for other subitems, suggesting that the cognitive component might primarily contribute to general fatigue in PwRMS. This finding indicates that the fatigue experienced by PwRMS may be driven by neurobiological mechanisms dependent on white matter changes, in contrast to the mechanisms underlying fatigue in HC.

Notably, both samples were comparable across all other measured variables. They were characterized by preserved cognitive capacity, minimal or no disability in PwRMS, and similar rates of depression and anxiety symptoms. These findings highlight a key association between white matter volume and fatigue, identifying specific brain regions involved in fatigue in PwRMS. For total fatigue, these areas include the left caudal anterior cingulate, left inferior frontal gyrus (pars triangularis), right banks of the superior temporal sulcus, left transverse temporal areas, right insula, left cerebellum, left entorhinal cortex, right lateral occipital, right rostral anterior cingulate, and left paracentral regions. Specifically, for cognitive fatigue, the areas identified primarily include the right and left banks of the superior temporal sulcus, the left lateral occipital, the right frontal pole, the left inferior frontal gyrus (pars orbitalis), and the bilateral areas of the cingulate cortex. These regions are critical components of networks involved in visual processing<sup>44</sup>, language<sup>45</sup>, cognitive control<sup>46–48</sup>, goal-directed decision-making<sup>49</sup>, social cognition<sup>50–52</sup>, sensorimotor integration<sup>53</sup>, and emotional and pain processing<sup>54</sup>.

On the other hand, in the case of PwRMS, changes in the specific superficial white matter fiber are identified through DTI<sup>55–58</sup>, specifically in FA, as reported by other studies<sup>59,60</sup>. Interestingly, the increase of FA in SWM related to fatigue was observed in PwRMS, in bundles associated with the left pars triangularis, one of the most relevant white matter regions that contribute more to the difference in the relation between white matter volumes and fatigue. This result supports the claim that fatigue in PwRMS may have a distinct neuroanatomical signature compared to fatigue in healthy individuals<sup>61</sup>.

Our findings extend prior research on fatigue in PwMS, with notable involvement in different white matter regions, such as the anterior cingulate cortex, a region consistently implicated in fatigue across neurological disorders<sup>59,62</sup>. Altered white matter volume in this area in PwRMS may reflect compromised functions such as error detection and performance monitoring<sup>63,64</sup>, as well as effort-based decision-making<sup>65,66</sup>, and pain processing<sup>67,68</sup>, in a similar way to that observed in other pathologies like schizophrenia<sup>69,70</sup>.

Observed alterations in the banks of the superior temporal sulcus contribute to understanding the disruptions in multimodal sensory integration<sup>71</sup> and social cognition<sup>72,73</sup>, presented in PwRMS. Further, differences in the transverse temporal regions, involved in basic auditory processing<sup>74</sup>, highlight alterations in speech

## White Matter Volumes Associated with Cognitive Fatigue

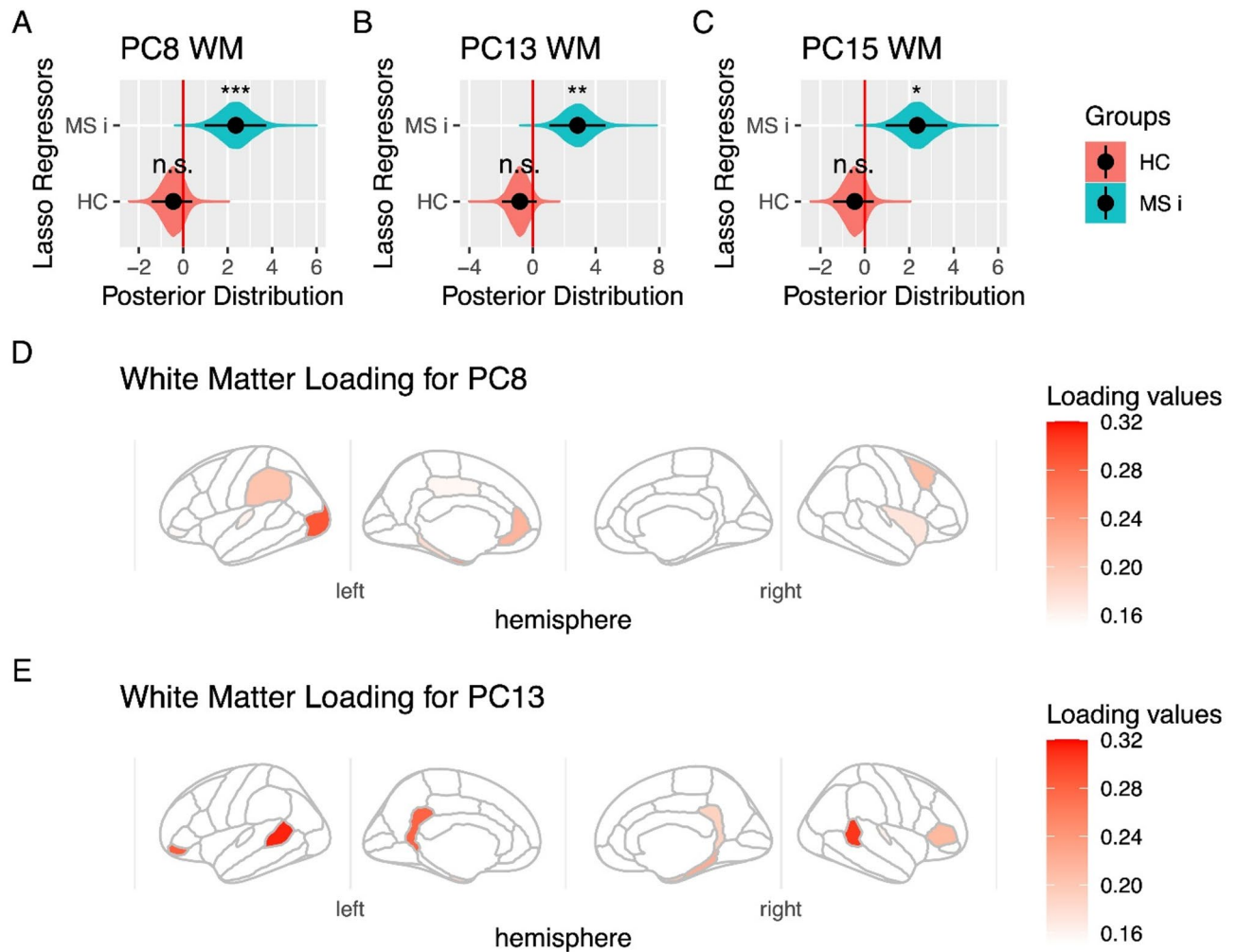


**Fig. 3.** White Matter Volumes Associated with Cognitive Fatigue, controlled for Physical Fatigue. **(A)** Principal Component #8 (PC8) demonstrated significant modulation in people with relapsing multiple sclerosis (PwRMS). They showed a significant interaction between PwRMS and healthy controls (HC) experiencing fatigue. **(B)** Principal Component #13 (PC13) demonstrated significant modulation in people with relapsing multiple sclerosis (PwRMS) and showed a significant interaction between PwRMS and healthy controls experiencing fatigue (HC). **(C)** Principal Component #15 (PC15) demonstrated significant modulation in people with relapsing multiple sclerosis (PwRMS) and showed a significant interaction between PwRMS and healthy controls experiencing fatigue (HC). **A–C:** The black dot indicates the median, the line shows the 95% high-density interval of the posterior distribution, and the shaded area represents the entire posterior distribution. **(D)** Loading for PC #8. The main white matter volumes are shown according to absolute values of loading of PC #8. In the *right hemisphere*: frontal pole (0.26), caudal middle frontal (0.2), insula (0.17). In the *left hemisphere*: lateral occipital (0.28), entorhinal (0.24), rostral anterior cingulate (0.21), supramarginal (0.2), parahippocampal (0.18). **(E)** Loading for PC13. The main white matter volumes are shown according to absolute values of loading of PC13. In the *right hemisphere*: banks of the superior temporal sulcus (0.30), parahippocampal (0.22), entorhinal (0.19), isthmus cingulate (0.18). In the *left hemisphere*: banks of the superior temporal sulcus (0.31), pars orbitalis (0.28), isthmus cingulate (0.27), temporal pole (0.21), pars triangularis (0.21), entorhinal (0.18). HC: Healthy control experience fatigue, MC i: Multiple sclerosis interaction, that means the difference in the correlation between HC and PwRMS, *rh*: *right hemisphere*, *lh*: *left hemisphere*. Statistical significance levels: *n.s.*, no significant difference; \* $p < 0.05$ ; \*\* $p < 0.01$ ; \*\*\* $p < 0.001$ .

comprehension and auditory attention<sup>75</sup> even at early stages of PwRMS. Differences in the insula's white matter volume indicate possible early effects on interoception, emotional processing, feedback monitoring processing<sup>76</sup>, and cognitive integration in PwRMS<sup>77</sup>. Altered white matter volume in the frontal pole in PwRMS may reflect compromised functions, such as goal-directed decision-making. Similarly, as observed in other studies, the

functional connectivity of monoamine circuits was significantly reduced in regions including the paracingulate gyrus, the frontal pole, the inferior frontal gyrus, and the middle frontal gyrus in cognitively fatigued PwMS<sup>64</sup>.

One region we highlight, both for its structural characteristics and connectivity, is the white matter in the pars triangularis and the SWM bundles traversing this area. This finding suggests that fatigue affects cognitive networks beyond motor function, aligning with recent findings that MS-related fatigue impacts language processing, sustained communication, social cognition, and executive functions, including inhibitory control and decision-making<sup>78–80</sup>. Nonetheless, the elevated FA associated with fatigue in SWM bundles connecting to the left pars triangularis may indicate early compensatory mechanisms aimed at offsetting changes in white matter regions associated with fatigue in PwMS. This finding aligns with the report by Buyukturkoglu et al.<sup>55</sup>, which demonstrated that patients in the early stages of MS exhibit significant changes in SWM bundles, including those connected to the insula, inferior frontal, orbitofrontal, superior and medial temporal, and pre- and post-central cortices, even prior pronounced structural and functional alterations emerge.

Our findings have several significant clinical implications. The observed differences in white matter volume suggest impairments in networks associated with sensory integration, language, decision-making, executive functions, and social cognition, all crucial for daily functioning<sup>81</sup> and closely linked to the quality of life in PwMS<sup>82</sup>. Early disruptions in white matter integrity and regional connectivity underscore the importance of vigilant monitoring of these patients. Additionally, there is a pressing need for interventions beyond fatigue's physical characteristics to address its diverse dimensions. Effective strategies should include cognitive rehabilitation to enhance cognitive function<sup>83</sup>, emotional support to manage mood disturbances<sup>84</sup>, and therapies to improve sensory integration<sup>85</sup>. However, given the limitations of current treatments, there remains ongoing debate about their efficacy<sup>86,87</sup>. For example, a randomized, placebo-controlled, crossover, double-blind trial by Nourbakhsh demonstrated that neither Amantadine nor Modafinil showed significant advantages over placebo in alleviating MS-related fatigue<sup>88</sup>. These findings highlight the need to explore other therapeutic approaches to manage fatigue better and improve the quality of life in this population.

In this context, our results provide insights that could guide future interventions to slow disease progression and reduce both the long-term effects of the disease and those related to aging. In recent years, non-invasive brain stimulation, informed by precise knowledge of functional and structural brain alterations, has shown the potential to alleviate various symptoms in brain pathologies<sup>89–91</sup>. These techniques have demonstrated their ability to produce changes in brain activity dependent on structural brain connectivity, leading to modulations in cognitive processing<sup>48,92,93</sup>. For example, studies found that interventions using transcranial direct current stimulation of the dorsolateral prefrontal cortex improved fatigue in PwMS<sup>94,95</sup>.

Comprehensive assessments for evaluating fatigue in PwMS are essential. These evaluations should encompass physical measures, cognitive evaluations, and emotional assessments to provide an integral view of the patient's experience with fatigue. Additionally, incorporating neuroinflammatory biomarkers specific to MS-related fatigue, such as cytokine levels, glial activation markers, and other indicators of neuroimmune activity, could enhance the precision of fatigue assessments and clarify the disease-related and non-disease-related contributions to fatigue in MS<sup>96</sup>.

Notably, while the scale employed in this study to assess subjective fatigue is validated for PwMS<sup>97</sup>, it demonstrates limited specificity in differentiating PwMS experiencing fatigue from HCs reporting fatigue. In contrast, structural white matter measures successfully distinguished these groups, emphasizing the utility of multimodal assessments in capturing fatigue-related differences. This result underscores the critical need for comprehensive, multimodal evaluations integrating diverse and relevant measures to optimize fatigue management in PwMS.

On the other hand, observing moderate fatigue in our HC cohort highlights the necessity of studying this phenomenon in non-clinical populations. Unexplained fatigue in otherwise healthy individuals has been associated with long-term risks of developing metabolic, immunological, or psychiatric dysfunctions<sup>22</sup>. These findings reinforce the importance of investigating the etiology and underlying mechanisms of fatigue in broader populations, which could provide valuable insights into early intervention and preventive health strategies.

Several limitations should be considered when interpreting our results. First, the cross-sectional design of this study limits our ability to establish causal relationships between white matter changes and the development of fatigue. Second, while our sample size was adequate for detecting group differences in the relation between white matter and fatigue, more extensive studies are needed to validate these findings and explore potential phenotypic variations. Furthermore, despite our samples being well matched in several clinical factors, the small sample size restricts our ability to control for possible confounding factors, including common comorbidities such as depression and anxiety<sup>98</sup>. Third, we did not include healthy subjects without fatigue symptoms, which prevents us from identifying specific mechanisms underlying fatigue in such individuals. Additionally, healthy controls with subjective fatigue were not assessed using the PASAT. This omission may limit comparing cognitive performance between groups and interpreting the relationship between fatigue and cognitive function. Future studies should consider including the PASAT for all participants to ensure comprehensive assessment and comparability across groups. In addition, focusing solely on structural changes may not fully capture the complexity of fatigue mechanisms, highlighting the need for multimodal imaging studies that include functional connectivity analyses, task-related fMRI, and EEG<sup>34</sup> to investigate additional phenotypes. Future research should investigate longitudinal changes in these brain regions as fatigue develops and fluctuates, explore the relationship between structural changes and functional connectivity<sup>99</sup>, examine how these structural differences relate to treatment response, and consider the impact of disease-modifying therapies on these white matter patterns.

In conclusion, this study provides evidence of distinct white matter volumetric patterns associated with fatigue in PwMS compared to HC experiencing fatigue. The involvement of regions essential for sensory integration, language, executive functions crucial for cognitive control, and social cognition suggests a unique neuroanatomical basis for fatigue in PwMS. These findings advance our understanding of fatigue pathophysiology in RMS and



underscore the importance of integrating additional measures, such as neuroinflammatory and stress-related measures, to enhance the specificity and sensitivity of fatigue assessments in both clinical and research settings, ultimately contributing to developing more targeted therapeutic approaches.

## Materials and methods

### Study design and participant selection

We conducted a cross-sectional study involving 32 participants with relapsing multiple sclerosis (PwRMS) and 29 healthy controls (HC) who presented similar levels of fatigue as measured by the Modified Fatigue Impact Scale (MFIS). For PwRMS, participants were enrolled in the Multiple Sclerosis Program at Pontificia Universidad Católica de Chile. A total of 77 PwRMS were initially assessed for eligibility. Patients were eligible if they had a clinically confirmed diagnosis of RMS, a brain MRI performed within six months before study enrollment, no relapses or disease progression in the past six months, and no history of other major neurological or psychiatric disorders. Additional inclusion criteria required participants to complete the MFIS for fatigue assessment to demonstrate preserved cognitive capacity as evaluated by the Paced Auditory Serial Addition Test (PASAT) and Symbol Digit Modalities Test (SDMT) (both  $\geq -1.5$  Z-score), have a null or mild level of disability<sup>100</sup> (Expanded Disability Status Scale (EDSS)  $\leq 3$ ), maintain usual medication for at least six months, and have no uncorrected visual deficits.

Of the initial cohort of 77 PwRMS, 26 individuals were excluded because they lacked a brain MRI performed within the required six-month timeframe, seven were excluded due to major neurological or psychiatric conditions such as addiction, bipolar disorder, or epilepsy, and 12 were excluded due to incomplete neuropsychological or MFIS evaluations.

For HC, clinical and demographic data and MRI outcomes were collected. HC participants were selected if they demonstrated fatigue levels similar to those of PwRMS as measured by the MFIS but had no medical history of major neurological, psychiatric, immunological, or metabolic disorders. Additional inclusion criteria included having a brain MRI performed within six months before study enrollment and no uncorrected visual deficits. The characteristics of the PwRMS and HC groups are shown in Table 1. Thus, HC participants were enrolled in Laboratorio de Neurociencia Social y Neuromodulación (NeuroCICS) at Centro de Investigación en Complejidad Social at Universidad del Desarrollo, Chile. We assessed the database of healthy participants from prior or concurrent MRI studies. The initial sample of 182 participants underwent a clinical evaluation, including a medical anamnesis and assessments using the GAD-7 and PHQ-9 scales before the MRI session of each respective study<sup>48,92,101</sup>. From this sample, we selected participants matched by age, sex, and schooling to the patient group. The MFIS (38 participants) further evaluated these chosen individuals for fatigue. Ultimately, a total of 29 healthy controls experiencing fatigue were recruited.

### Ethics declarations

All participants gave informed consent, and all experimental procedures were approved by the Ethical Committee for Health Sciences at Pontificia Universidad Católica de Chile, Chile (ID: 220711001). These consent processes and all procedures complied with Chilean national legislation, institutional guidelines, and the Declaration of Helsinki.

### MRI outcome measures

The MRI protocol for PwMS was conducted as part of the Multiple Sclerosis Program within the Faculty of Medicine at the Pontifical Catholic University of Chile, according to the policies of the Chilean Ministry of Health. These were performed on Philips 3 T scanners using standardized three-dimensional fluid-attenuated inversion recovery (3D FLAIR) and 3D T1 (MPRAGE [magnetization-prepared rapid gradient-echo imaging]) acquisition sequences. Both structural and functional images were acquired on a Philips Ingenia 3 T MRI scanner. T1 weighted 3D images (repetition time [TR] 7.8 s, echo time [TE] 3.6 ms, flip angle 8°, SENSE factor 2.5, acquisition time 4 min 8 s) and a sagittal 3D fluid attenuation inversion recovery (FLAIR) (TR 4800 ms, TE 290 ms, acquisition time 4 min 33 s).

The MRI protocol for HC was conducted using Siemens Skyra 3 T scanners and included (i) a sagittal 3D anatomical MPRAGE T1-weighted imaging (TR/echo time [TE] = 2530/2.19 ms, inversion time [TI] = 1100 ms, flip angle = 7°;  $1 \times 1 \times 1$  mm<sup>3</sup> voxels), (ii) a sagittal 3D anatomical SPC T2-weighted (TR/TE = 3200/412 ms, flip angle = 120°; echo train length [ETL] = 258;  $1 \times 1 \times 1$  mm<sup>3</sup> voxels), (iii) a sagittal 3D FLAIR imaging (TR/TE = 5000/388 ms, TI = 1800 ms, ETL = 251; flip angle = 120°, 1-mm slice thickness,  $1 \times 1 \times 1$  mm<sup>3</sup> voxels), (iv) an axial 3D echo-planar imaging (EPI) (TR/TE = 8600/95 ms,  $2 \times 2 \times 2$  mm<sup>3</sup> voxels, flip angle = 90°) with diffusion gradients applied in 60 non-collinear directions and two optimized b factors ( $b_1 = 0$  and  $b_2 = 1000$  s/mm<sup>2</sup>) with two repetitions.

### Participant-reported outcomes

For all participants, as in prior work<sup>101</sup>, the presence of anxiety symptoms was assessed using the Spanish version of the GAD-7<sup>102</sup>. The GAD-7 is a brief self-report scale comprising seven items designed to identify probable cases of Generalized Anxiety Disorder based on the diagnostic criteria of the Diagnostic and Statistical Manual of Mental Disorders - fourth edition (DSM-IV). The assessment of depressive symptoms was conducted using the Spanish version of the PHQ-9<sup>103</sup>. The PHQ-9 consists of 9 items that assess the presence of depressive symptoms (corresponding to DSM-IV criteria) experienced in the past 2 weeks. Fatigue was evaluated using the MFIS<sup>104,105</sup>, a 21-item self-reported measure of fatigue that assesses the impact on psychosocial, physical, and cognitive function. The total score ranges from 0 to 84 (the higher the score, the worse the fatigue). MFIS items can be aggregated into three subscales: cognitive (score range 0–40), physical (score range 0–36), and psychosocial (score range 0–8). The MFIS is a valid and reliable tool for assessing fatigue, has a low floor and

ceiling effect, and captures both physical and cognitive aspects of fatigue<sup>105</sup>. It is the recommended tool for assessing fatigue in clinical practice and research in PwMS<sup>106</sup>.

### Z-score calculation for cognitive tests

Z-scores for the Paced Auditory Serial Addition Test (PASAT)<sup>107</sup> and the Symbol Digit Modalities Test (SDMT)<sup>108</sup> were calculated to standardize individual performance relative to the distribution of a normative reference population. Raw scores were obtained for each test based on the participants' performance. The Z-score for each individual was computed using the formula:

$$Z = (X - \mu) / \sigma$$

Where X is the participant's raw score,  $\mu$  is the mean score of the normative population, and  $\sigma$  is the standard deviation of the normative population. The normative data for PASAT and SDMT were derived from established datasets that account for demographic factors such as age, sex, and education level. Adjustments were made when necessary to match the demographic characteristics of the study population. This standardization enabled direct comparison of cognitive performance across participants and between groups.

### Descriptive analysis

All variables in the study were reported as median and interquartile range (IQR). The median provides a measure of central tendency, representing the middle value of a variable when the data is ordered from lowest to highest. The IQR measures statistical dispersion, defined as the range between the 75 th percentile (Q3) and the 25 th percentile (Q1), capturing the spread of the middle 50% of the data.

To calculate these values, we used the median() and IQR() functions in R. For each group (PwRMS and healthy controls), the median and IQR were computed for variables such as Age, MFIS, SDMT, PASAT, and others included in the analysis. These measures were chosen due to the non-normal distribution of several variables, making the median and IQR more appropriate measures of central tendency and variability than the mean and standard deviation. These values were used to summarize participant characteristics and provide a robust data description. The results for the PwRMS and healthy control groups are reported separately in Table 1.

### Brain segmentation volumes and cortical thickness measurements

In the first step, we segmented brain areas and consulted volumes. Structural Image processing was conducted using the first two steps of the Human Connectome Project (HCP) pipeline, as described in our prior works<sup>101,109</sup>, and detailed elsewhere<sup>110</sup>. Briefly, the "PreFreeSurfer" phase generated an undistorted native structural volume space, aligned T1-weighted and T2-weighted images, corrected bias fields derived from both images, and registered the native space to the common MNI coordinate space using a rigid affine registration, and then, a non-linear registration to standard space. Utilizing FreeSurfer version 6, the "FreeSurfer" stage conducted volume segmentation and cortical surface reconstructions, including delineation of the "white" (gray/white matter boundary) and "pial" (gray/cerebrospinal fluid boundary) surfaces, followed by registration to a common template (fsaverage).

In the second step, we conducted a PCA to study the relationship between cortical and subcortical gray matter volumes, white matter volumes, and self-reported global fatigue from the MFIS in PwRMS and HC. This analysis was performed on three groups of regions: subcortical gray matter, white matter, and cortical gray matter. The latter was segmented using the Desikan–Killiany atlas<sup>111</sup>. PCA allowed us to reduce the complexity of volumetric data while retaining the most variance, facilitating an exploration of the associations between brain structures and fatigue scores across the study groups. This approach has been used for complex data from MRI and integrated modalities by other groups<sup>112</sup>. Additionally, as PCA generates orthogonal components, the resulting principal components can be effectively utilized in linear regression analyses such as LASSO. This approach is particularly advantageous because LASSO regression helps control for multicollinearity among predictors, ensuring the model remains robust and interpretable (see above). Moreover, using PCA-derived components allows for multiple comparison corrections, reducing the risk of Type I errors when assessing associations between brain structures and fatigue scores<sup>43</sup>. Additionally, to minimize potential biases arising from acquisition on different scanners, which the standardized HCP algorithm cannot fully correct, we avoided direct comparisons of MRI measures between groups. Instead, all models focus on testing group differences in the relationship between MRI measures and clinical variables (see below).

In the third step, we applied a Bayesian Least Absolute Shrinkage and Selection Operator (LASSO) and Bayesian Spike-and-Slab Lasso (SSL) linear regression models using R (A language and environment for statistical computing) in conjunction with the Just Another Gibbs Sampler (JAGS: A program for analysis of Bayesian graphical models using Gibbs sampling). LASSO and SSL offer robust frameworks for addressing the challenges associated with multiple comparisons in regression analysis. Their ability to perform automatic feature selection while controlling for overfitting makes them tools for high-dimensional data analysis. This method enabled the analysis of compositional data, improving the accuracy of parameter estimation and offering more profound insights into the relationships between the compositional predictors—namely, the PCA of cortical and subcortical gray matter and white matter volumes—and the outcome variable of fatigue. Since compositional data inherently reflect the relative nature of its components, analyzing them allows for better differentiation of ratings and reduces response biases. This approach is effective whether all components contributing to the total are fully quantified or only a subset is included<sup>113</sup>. Thus, these methods mitigate the type I error rate through its inherent feature selection process, as it tends to include only a subset of statistically significant predictors, thus reducing the number of tests conducted on non-informative variables<sup>114</sup>. For these analyses, we used the first 10 components for subcortical segmentation and the first 20 for white and cortical gray matter.

For both LASSO and SSL, we used the following statistical model:

$$\text{MFIS} \sim \beta_0 + \beta_1 \text{MS} + \beta_{2,i} \text{PCi} + \beta_{3,i} \text{PCi} \cdot \text{MS} + \beta_{4,g} \text{TIV} \quad (1)$$

In this equation,  $\beta_0$  represents the intercept, while  $\beta_1$  indicates the slope corresponding to the difference in the test associated with the diagnosis of Multiple Sclerosis. The term  $\beta_{2,i}$  represents the slope corresponding to principal component  $i$  ( $i = 1$  to 10 for subcortical gray matter, and  $i = 1$  to 20 for the white and cortical gray matter). The term  $\beta_{3,i}$  represents the slope corresponding to the interaction between each principal component  $i$  and the diagnosis of multiple sclerosis. This term represents the difference in the relationship between each component and fatigue across groups. Additionally, we can compute the correlation between each component and fatigue within patient groups by summing the slopes and making statistical inferences using this posterior distribution (e.g., for PC  $i$ :  $\beta_{3,i} + \beta_{2,i}$ , see below). The term  $\beta_{4,g}$  represents the relationship between fatigue and total intracranial volume separated by each group ( $g$ ), used as a control. To control for depressive and anxiety symptoms, we included the PHQ-9 and GAD-7 scores ( $t$ ) in the regression model, accounting for these effects with the  $\beta_{5,t}$  term. Similarly, in the analysis of cognitive fatigue, we controlled for physical fatigue by including the physical fatigue score ( $t$ ) using the  $\beta_{5,t}$  term.

Inferences for significant regressors were assessed using the 95% highest density interval (HDI) of the posterior distribution. A  $p$ -value equivalent ( $p_{\text{MCMC}}$ ) was calculated by comparing Markov Chain Monte Carlo (MCMC) samples against a reference value of zero.  $P$ -values below 0.05 were considered statistically significant, and all comparisons were two-tailed. Statistical analyses were conducted using R (version 4.2.1).

### Connectivity MRI analysis

The diffusion imaging was processed using MRtrix3 software<sup>115</sup>. The first stage of the process was to apply a pre-processing pipeline, which involved several steps designed to enhance image quality and reduce the impact of artifacts. These steps included image denoising, correction of Gibbs ringing, motion and eddy current distortion correction, and N4 bias field correction. The pre-processed diffusion images were used to calculate the Diffusion Tensor Imaging (DTI) model and extract the fractional anisotropy (FA). A deterministic tractography algorithm (*Tensor\_det*) with Anatomically Constrained Tractography (ACT) was then applied using the following parameters: angular threshold = 60°, step size = 0.2 mm, minimum length = 25 mm, maximum length = 250 mm, and FA threshold = 0.06 (adjusted to 0.03 when ACT is used). The T1w image was coregistered to the diffusion-weighted imaging (DWI) space using FSL's FLIRT tool, with 6 degrees of freedom (DOF) rigid-body transformation. With the T1w image aligned to the diffusion space, subject parcellation (Desikan atlas) was performed using the FreeSurfer *MRI\_SynthSeg* tool.

Since the diffusion data for PwRMS and healthy controls experiencing fatigue were acquired in different centers using different scanners, direct comparison between the centers was impossible; any significant results could be attributed to scanner differences rather than biological factors. Therefore, two different analyses were conducted solely among PwRMS, focusing on the relationship between fatigue scores and FA values within these fiber bundles.

### Mean FA measures of ROI tracts

Using the tractogram (DWI space) and the cortical parcellation, a tractography-based connectome was generated using MRtrix3 (*tck2connectome* command). Then, we selected the fibers that connect, at both ends, the regions that show a difference in white matter (WM) thickness that were previously calculated (*connectome2 tck*). These connections comprise short association fibers of the superficial white matter (SWM)<sup>116,117</sup>. The SWM refers to the highly complex layer of WM immediately deep into the cortical GM and above the deep WM. The SWM maintains the thalamocortical connections and is a necessary pathway for all axons passing through the GM and WM. Despite its characteristics, the SWM is one of the least understood regions of the brain. We filtered all fibers with lengths higher than 80 mm from the extracted connections to ensure that we analyze only these short fibers and remove noisy fibers. These segmented tracts were then used to conduct a statistical analysis based on the mean FA measures in these regions (Fig. 4).

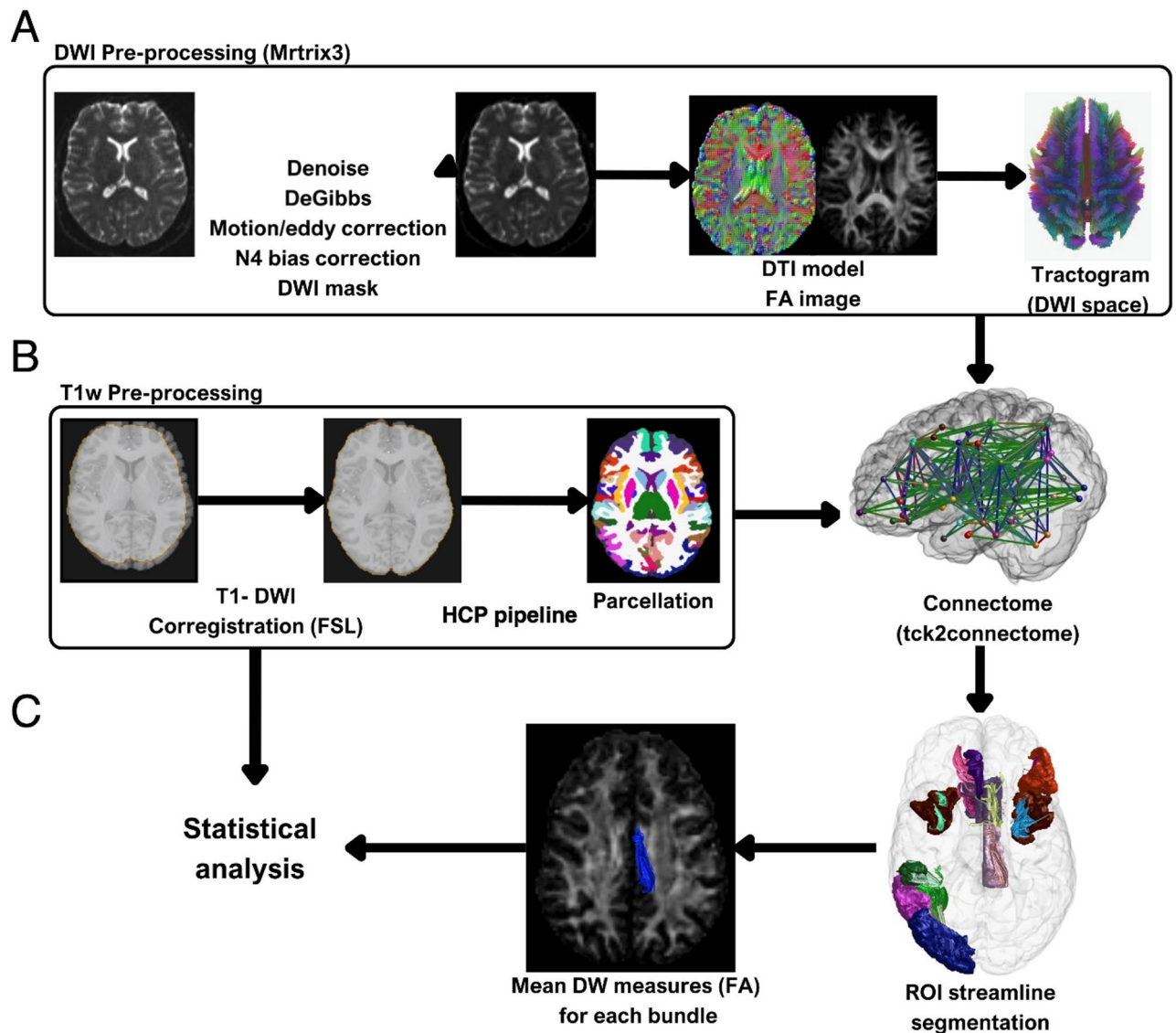


**Fig. 4.** Connectivity analysis methodology. (A) Raw diffusion-weighted images (DWI) undergo various pre-processing steps to enhance image quality. Following the pre-processing, DTI, FA, and DWI mask images are generated. These outputs are used to create a deterministic whole-brain tractography dataset. (B) The T1w image is co-registered to the DWI space. After co-registration, the cortical parcellation is generated using the HCP pipeline, which uses the Freesurfer *mri\_syntheseg* algorithm based on the Desikan Killiany atlas<sup>111</sup>. (C) A structural connectome is generated Using the cortical parcellation and the tractogram to identify and segment the fibers connecting the specific ROIs. The mean FA values of these ROI tracts are then calculated and used for statistical analysis.

### Data availability

The minimal data sets to reproduce the results were available in the GitHub repository ([https://github.com/neurocics/Figueroa-Vargas\\_Navarrete\\_2025\\_Scientific\\_Reports](https://github.com/neurocics/Figueroa-Vargas_Navarrete_2025_Scientific_Reports)). All codes are available in the GitHub repository ([https://github.com/neurocics/Figueroa-Vargas\\_Navarrete\\_2025\\_Scientific\\_Reports](https://github.com/neurocics/Figueroa-Vargas_Navarrete_2025_Scientific_Reports)). For further inquiries, please contact Pablo Billeke at pbilleke@udd.cl and Alejandra Figueroa-Vargas at amfigueroa@udd.cl.

Received: 8 November 2024; Accepted: 6 May 2025

Published online: 12 May 2025

### References

- Walton, C. et al. Rising prevalence of multiple sclerosis worldwide: insights from the atlas of MS, third edition. *Mult Scler. J.* **26**, 1816–1821 (2020).
- Thompson, A. J., Baranzini, S. E., Geurts, J., Hemmer, B. & Ciccarelli, O. *Multiple Scler. Lancet* **391**, 1622–1636 (2018).
- Kampaite, A. et al. Brain connectivity changes underlying depression and fatigue in relapsing-remitting multiple sclerosis: A systematic review. *PLOS ONE*. **19**, e0299634 (2024).



4. Meijboom, R. et al. Fatigue in early multiple sclerosis: MRI metrics of neuroinflammation, relapse and neurodegeneration. *Brain Commun.* **6**, fcae278 (2024).
5. Ahvenjärvi, H. et al. Fatigue and health-related quality of life depend on the disability status and clinical course in RRMS. *Mult Scler. Relat. Disord.* **77**, 104861 (2023).
6. Ramirez, A. O. et al. Prevalence and burden of multiple sclerosis-related fatigue: a systematic literature review. *BMC Neurol.* **21**, 468 (2021).
7. Bass, A. D. et al. Multiple sclerosis impact on daily activities, emotional Well-Being, and relationships: the global VsMS™ survey. *Int. J. MS Care.* **22**, 158–164 (2019).
8. Sandry, J., Genova, H. M., Dobryakova, E., DeLuca, J. & Wylie, G. Subjective cognitive fatigue in multiple sclerosis depends on task length. *Front. Neurol.* **5**, 214 (2014).
9. Larson, R. D. Psychometric properties of the modified fatigue impact scale. *Int. J. MS Care.* **15**, 15–20 (2013).
10. López-Muguruza, E. & Matute, C. Alterations of oligodendrocyte and Myelin energy metabolism in multiple sclerosis. *Int. J. Mol. Sci.* **24**, 12912 (2023).
11. Kirmaci, Z. İ. K. et al. Muscle architecture and its relationship with lower extremity muscle strength in multiple sclerosis. *Acta Neurol. Belg.* **122**, 1521–1528 (2022).
12. Khan, Z., Mehan, S., Gupta, G. D. & Narula, A. S. Immune system dysregulation in the progression of multiple sclerosis: molecular insights and therapeutic implications. *Neuroscience* **548**, 9–26 (2024).
13. Adibi, I. et al. Multiple sclerosis-related fatigue lacks a unified definition: A narrative review. *J. Res. Méd Sci. : Off J. Isfahan Univ. Méd Sci.* **27**, 24 (2022).
14. Patejdl, R. & Zettl, U. K. The pathophysiology of motor fatigue and fatigability in multiple sclerosis. *Front. Neurol.* **13**, 891415 (2022).
15. Hammam, N. et al. Fatigue in rheumatoid arthritis patients: association with Sleep quality, mood status, and disease activity. *Reum Clínica.* **16**, 339–344 (2020).
16. Tarazi, M., Gaffney, R. G., Pearson, D., Kushner, C. J. & Werth, V. P. Fatigue in systemic lupus erythematosus and other autoimmune skin diseases. *Br. J. Dermatol.* **180**, 1468–1472 (2019).
17. Raveendran, A. V., Jayadevan, R., Sashidharan, S. & Long, C. O. V. I. D. An overview. *Diabetes Metab. Syndr. : Clin. Res. Rev.* **15**, 869–875 (2021).
18. Maqbal, M. A., Sinani, M. A., Naamani, Z. A., Badi, K. A. & Tanash, M. I. Prevalence of fatigue in patients with cancer: A systematic review and Meta-Analysis. *J. Pain Symptom Manag.* **61**, 167–189e14 (2021).
19. Yoon, J. H. et al. The demographic features of fatigue in the general population worldwide: a systematic review and meta-analysis. *Front. Public. Heal.* **11**, 1192121 (2023).
20. Nicholson, K., Stewart, M. & Thind, A. Examining the symptom of fatigue in primary care: a comparative study using electronic medical records. *J. Innov. Heal Inf.* **22**, 235–243 (2015).
21. Boulosa, D. A. & Nakamura, F. Y. The evolutionary significance of fatigue. *Front. Physiol.* **4**, 309 (2013).
22. Nijrolder, L., van der Windt, D., de Vries, H. & van der Horst, H. Diagnoses during follow-up of patients presenting with fatigue in primary care. *Can. Méd Assoc. J.* **181**, 683–687 (2009).
23. Maisel, P. & Baum, E. Donner-Banzhoff, N. Fatigue as the chief complaint. *Dtsch. Aerzteblatt Online.* **118**, 566–576 (2021).
24. Li, H., Zhao, J., Liang, J. & Song, X. Exploring causal effects of smoking and alcohol related lifestyle factors on self-report tiredness: A Mendelian randomization study. *PLOS ONE.* **18**, e0287027 (2023).
25. da Mesquita, R. Clinical manifestations of COVID-19 in the general population: systematic review. *Wien Klin. Wochenschr.* **133**, 377–382 (2021).
26. Manjaly, Z. M. et al. Pathophysiological and cognitive mechanisms of fatigue in multiple sclerosis. *J. Neurol. Neurosurg. Psychiatry.* **90**, 642 (2019).
27. Jakimovski, D. et al. *Multiple Scler. Lancet* **403**, 183–202 (2024).
28. Filippi, M. et al. Association between pathological and MRI findings in multiple sclerosis. *Lancet Neurol.* **18**, 198–210 (2019).
29. Wattjes, M. P. et al. 2021 MAGNIMS-CMSC-NAIMS consensus recommendations on the use of MRI in patients with multiple sclerosis. *Lancet Neurol.* **20**, 653–670 (2021).
30. Filippi, M. et al. Present and future of the diagnostic work-up of multiple sclerosis: the imaging perspective. *J. Neurol.* **270**, 1286–1299 (2023).
31. York, E. N. et al. Longitudinal microstructural MRI markers of demyelination and neurodegeneration in early relapsing-remitting multiple sclerosis: magnetisation transfer, water diffusion and g-ratio. *NeuroImage: Clin.* **36**, 103228 (2022).
32. Galazzo, I. B. et al. Unraveling the MRI-Based microstructural signatures behind primary progressive and Relapsing-Remitting multiple sclerosis phenotypes. *J. Magn. Reson. Imaging.* **55**, 154–163 (2022).
33. Shi, Z. et al. Microstructural alterations in different types of lesions and their perilesional white matter in relapsing-remitting multiple sclerosis based on diffusion kurtosis imaging. *Mult Scler. Relat. Disord.* **71**, 104572 (2023).
34. Figueroa-Vargas, A. et al. Frontoparietal connectivity correlates with working memory performance in multiple sclerosis. *Sci. Rep.* **10**, 9310 (2020).
35. Wenger, A. L. et al. An investigation of the association between focal damage and global network properties in cognitively impaired and cognitively preserved patients with multiple sclerosis. *Front. Neurosci.* **17**, 1007580 (2023).
36. Hogestol, E. A. et al. Symptoms of fatigue and depression is reflected in altered default mode network connectivity in multiple sclerosis. *PLoS ONE.* **14**, e0210375 (2019).
37. Danciu, I. et al. Understanding the mechanisms of fatigue in multiple sclerosis: linking interoception, metacognition and white matter dysconnectivity. *Brain Commun.* **6**, fcae292 (2024).
38. Baran, T. M., Zhang, Z., Anderson, A. J., McDermott, K. & Lin, F. Brain structural connectomes indicate shared neural circuitry involved in subjective experience of cognitive and physical fatigue in older adults. *Brain Imaging Behav.* **14**, 2488–2499 (2020).
39. Román, C. A. F., Wylie, G. R., DeLuca, J. & Yao, B. Associations of white matter and basal ganglia microstructure to cognitive fatigue rate in multiple sclerosis. *Front. Neurol.* **13**, 911012 (2022).
40. Margoni, M. et al. Resting state functional connectivity modifications in monoaminergic circuits underpin fatigue development in patients with multiple sclerosis. *Mol. Psychiatry.* **29**, 2647–2656 (2024).
41. Herring, T. E. et al. Differences in correlates of fatigue between relapsing and progressive forms of multiple sclerosis. *Mult Scler. Relat. Disord.* **54**, 103109 (2021).
42. Bayas, A., Berthele, A., Hemmer, B., Warnke, C. & Wildemann, B. Controversy on the treatment of multiple sclerosis and related disorders: positional statement of the expert panel in charge of the 2021 DGN guideline on diagnosis and treatment of multiple sclerosis, neuromyelitis Optica spectrum diseases and MOG-IgG-associated disorders. *Neurol. Res. Pr.* **3**, 45 (2021).
43. Guha, A. et al. Topographies of cortical and subcortical volume loss in HIV and aging in the cART era. *JAIDS J. Acquir. Immune Defic. Syndr.* **73**, 374–383 (2016).
44. Takemura, H. et al. A prominent vertical occipital white matter fasciculus unique to primate brains. *Curr. Biol.* **34**, 3632–3643e4 (2024).
45. Bulut, T. Domain-general and domain-specific functional networks of Broca's area underlying Language processing. *Brain Behav.* **13**, e3046 (2023).
46. Orr, C. & Hester, R. Error-related anterior cingulate cortex activity and the prediction of conscious error awareness. *Front. Hum. Neurosci.* **6**, 177 (2012).

47. Zamorano, F. et al. Lateral prefrontal Theta oscillations reflect proactive cognitive control impairment in males with attention deficit hyperactivity disorder. *Front. Syst. Neurosci.* **14**, 37 (2020).
48. Martínez-Molina, M. P. et al. Lateral prefrontal theta oscillations causally drive a computational mechanism underlying conflict expectation and adaptation. *Nat. Commun.* **15**, 9858 (2024).
49. Hogeveen, J. et al. What does the frontopolar cortex contribute to Goal-Directed cognition and action?? *J. Neurosci.* **42**, 8508–8513 (2022).
50. Deen, B., Koldewyn, K., Kanwisher, N. & Saxe, R. Functional organization of social perception and cognition in the superior Temporal sulcus. *Cereb. Cortex.* **25**, 4596–4609 (2015).
51. Kausel, L., Michon, M., Soto-Icaza, P. & Aboitiz, F. A multimodal interface for speech perception: the role of the left superior Temporal sulcus in social cognition and autism. *Cereb. Cortex.* **34**, 84–93 (2024).
52. Lavin, C., Soto-Icaza, P., López, V. & Billeke, P. Another in need enhances prosociality and modulates frontal theta oscillations in young adults. *Front. Psychiatry.* **14**, 1160209 (2023).
53. Venezia, J. H. et al. Auditory, visual and audiovisual speech processing streams in superior Temporal sulcus. *Front. Hum. Neurosci.* **11**, 174 (2017).
54. Coffeen, U. et al. The role of the insular cortex and serotonergic system in the modulation of Long-Lasting nociception. *Cells* **13**, 1718 (2024).
55. Buyukturkoglu, K. et al. Machine learning to investigate superficial white matter integrity in early multiple sclerosis. *J. Neuroimaging.* **32**, 36–47 (2022).
56. Cavallari, M. et al. Fatigue predicts disease worsening in relapsing-remitting multiple sclerosis patients. *Mult Scler. J.* **22**, 1841–1849 (2016).
57. Zhou, F. et al. Altered Inter-Subregion connectivity of the default mode network in relapsing remitting multiple sclerosis: A functional and structural connectivity study. *PLoS ONE* **9**, e101198 (2014).
58. Zhou, F. et al. Intrinsic functional plasticity of the thalamocortical system in minimally disabled patients with Relapsing-Remitting multiple sclerosis. *Front. Hum. Neurosci.* **10**, 2 (2016).
59. Andreasen, A. K. et al. Regional brain atrophy in primary fatigued patients with multiple sclerosis. *NeuroImage* **50**, 608–615 (2010).
60. Pardini, M., Bonzano, L., Mancardi, G. L. & Roccatagliata, L. Frontal networks play a role in fatigue perception in multiple sclerosis. *Behav. Neurosci.* **124**, 329–336 (2010).
61. Nakagawa, S. et al. Basal ganglia correlates of fatigue in young adults. *Sci. Rep.* **6**, 21386 (2016).
62. Pezzetta, R. et al. Combined EEG and immersive virtual reality unveil dopaminergic modulation of error monitoring in Parkinson's disease. *Npj Park 's Dis.* **9**, 3 (2023).
63. López-Góngora, M. et al. Neurophysiological evidence of compensatory brain mechanisms in Early-Stage multiple sclerosis. *PLoS ONE.* **10**, e0136786 (2015).
64. Cercignani, M. et al. Cognitive fatigue in multiple sclerosis is associated with alterations in the functional connectivity of monoamine circuits. *Brain Commun.* **3**, fcab023 (2021).
65. Muhlert, N. et al. The grey matter correlates of impaired decision-making in multiple sclerosis. *J. Neurol. Neurosurg. Psychiatry.* **86**, 530 (2015).
66. Brassard, S. L., Liu, H., Dosanjh, J., MacKillop, J. & Balodis, I. Neurobiological foundations and clinical relevance of effort-based decision-making. *Brain Imaging Behav.* 1–30. <https://doi.org/10.1007/s11682-024-00890-x> (2024).
67. Heitmann, H. et al. Fatigue, depression, and pain in multiple sclerosis: how neuroinflammation translates into dysfunctional reward processing and anhedonic symptoms. *Mult Scler. J.* **28**, 1020–1027 (2020).
68. Brown, F. S. et al. Pain and cognitive performance in adults with multiple sclerosis: A systematic review. *Mult Scler. Relat. Disord.* **71**, 104584 (2023).
69. Polli, F. E. et al. Reduced error-related activation in two anterior cingulate circuits is related to impaired performance in schizophrenia. *Brain* **131**, 971–986 (2008).
70. Billeke, P. et al. Paradoxical expectation: oscillatory brain activity reveals social interaction impairment in schizophrenia. *Biol. Psychiatry.* **78**, 421–431 (2015).
71. Achiron, A. et al. Superior Temporal gyrus thickness correlates with cognitive performance in multiple sclerosis. *Brain Struct. Funct.* **218**, 943–950 (2013).
72. Yokote, H., Okano, K. & Toru, S. Theory of Mind and its neuroanatomical correlates in people with multiple sclerosis. *Mult Scler. Relat. Disord.* **55**, 103156 (2021).
73. Billeke, P., Zamorano, F., Cosmelli, D. & Aboitiz, F. Oscillatory brain activity correlates with risk perception and predicts social decisions. *Cereb. Cortex.* **23**, 2872–2883 (2013).
74. Nourski, K. V. et al. Processing of auditory novelty in human cortex during a semantic categorization task. *Hear. Res.* **444**, 108972 (2024).
75. Carter, S. L. et al. Differences in resting state functional connectivity relative to multiple sclerosis and impaired information processing speed. *Front. Neurol.* **14**, 1250894 (2023).
76. Billeke, P. et al. Human anterior Insula encodes performance feedback and relays prediction error to the medial prefrontal cortex. *Cereb. Cortex.* **30**, 4011–4025 (2020).
77. Salamone, P. C. et al. Altered neural signatures of interoception in multiple sclerosis. *Hum. Brain Mapp.* **39**, 4743–4754 (2018).
78. Roheger, M., Grothe, L., Hasselberg, L., Grothe, M. & Meinzer, M. A systematic review and meta-analysis of socio-cognitive impairments in multiple sclerosis. *Sci. Rep.* **14**, 7096 (2024).
79. Chen, M. H., DeLuca, J., Genova, H. M., Yao, B. & Wylie, G. R. Cognitive fatigue is associated with altered functional connectivity in interoceptive and reward pathways in multiple sclerosis. *Diagnostics* **10**, 930 (2020).
80. Ratzan, A. S. et al. Characterizing the Extended Language Network in Individuals with Multiple Sclerosis. *medRxiv* <https://doi.org/10.1101/2023.08.30.23294843> (2023).
81. Shah, A. Fatigue in multiple sclerosis. *Phys. Med. Rehabilitation Clin. North. Am.* **20**, 363–372 (2009).
82. Ziemssen, T. Multiple sclerosis beyond EDSS: depression and fatigue. *J. Neurol. Sci.* **277**, S37–S41 (2009).
83. Chen, M. H., Chiaravalloti, N. D. & DeLuca, J. Neurological update: cognitive rehabilitation in multiple sclerosis. *J. Neurol.* **268**, 4908–4914 (2021).
84. Mohr, D. C., Hart, S. L. & Goldberg, A. Effects of treatment for depression on fatigue in multiple sclerosis. *Psychosom. Med.* **65**, 542–547 (2003).
85. Gandolfi, M. et al. Sensory integration balance training in patients with multiple sclerosis: A randomized, controlled trial. *Mult Scler. J.* **21**, 1453–1462 (2014).
86. NG220, guideline & NICE. Multiple Sclerosis in Adults: Management. (2022).
87. Braley, T. J. & Chervin, R. D. Fatigue in multiple sclerosis: mechanisms, evaluation, and treatment. *Sleep* **33**, 1061–1067 (2010).
88. Nourbakhsh, B. et al. Safety and efficacy of Amantadine, Modafinil, and methylphenidate for fatigue in multiple sclerosis: a randomised, placebo-controlled, crossover, double-blind trial. *Lancet Neurol.* **20**, 38–48 (2021).
89. Figueroa-Vargas, A. et al. The effect of a cognitive training therapy based on stimulation of brain oscillations in patients with mild cognitive impairment in a Chilean sample: study protocol for a phase IIb, 2 × 3 mixed factorial, double-blind randomised controlled trial. *Trials* **25**, 1–14 (2024).

90. Soto-Icaza, P. et al. Oscillatory activity underlying cognitive performance in children and adolescents with autism: a systematic review. *Front. Hum. Neurosci.* **18**, 1320761 (2024).
91. Burton, C. Z. et al. Combined cognitive training and transcranial direct current stimulation in neuropsychiatric disorders: A systematic review and Meta-analysis. *Biol. Psychiatry: Cogn. Neurosci. Neuroimaging.* **8**, 151–161 (2023).
92. Valdebenito-Oyarzo, G. et al. The parietal cortex has a causal role in ambiguity computations in humans. *PLOS Biol.* **22**, e3002452 (2024).
93. Momi, D. et al. Perturbation of resting-state network nodes preferentially propagates to structurally rather than functionally connected regions. *Sci. Rep.* **11**, 12458 (2021).
94. Mortezaejad, M., Ehsani, F., Masoudian, N., Zoghi, M. & Jaberzadeh, S. Comparing the effects of multi-session anodal transcranial direct current stimulation of primary motor and dorsolateral prefrontal cortices on fatigue and quality of life in patients with multiple sclerosis: a double-blind, randomized, sham-controlled trial. *Clin. Rehabilitation.* **34**, 1103–1111 (2020).
95. Chalah, M. A. et al. Fatigue in multiple sclerosis: neural correlates and the role of Non-Invasive brain stimulation. *Front. Cell. Neurosci.* **9**, 460 (2015).
96. Filippo, M. D. et al. Fluid biomarkers in multiple sclerosis: from current to future applications. *Lancet Reg. Heal - Eur.* **44**, 101009 (2024).
97. Amtmann, D. et al. Comparison of the psychometric properties of two fatigue scales in multiple sclerosis. *Rehabilitation Psychol.* **57**, 159–166 (2012).
98. Boeschoten, R. E. et al. Prevalence of depression and anxiety in multiple sclerosis: A systematic review and meta-analysis. *J. Neurol. Sci.* **372**, 331–341 (2017).
99. Simpson, A. C. et al. Structural MRI measures are associated with fatigue severity and persistence in a large, real-world cohort of people with multiple sclerosis. *Mult Scler. J.* **30**, 738–746 (2024).
100. Kurtzke, J. F. Rating neurologic impairment in multiple sclerosis an expanded disability status scale (EDSS). *Neurology* **33**, 1444–1444 (1983).
101. Kausel, L. et al. Patients recovering from COVID-19 who presented with anosmia during their acute episode have behavioral, functional, and structural brain alterations. *Sci. Rep.* **14**, 19049 (2024).
102. Crockett, M. A., Martínez, V. & Ordóñez-Carrasco, J. L. Propiedades Psicométricas de La Escala generalized anxiety disorder 7-Item (GAD-7) En Una muestra comunitaria de adolescentes En Chile. *Rev. Médica Chile.* **150**, 458–464 (2022).
103. Borghero, F. et al. Tamizaje de episodio depresivo En adolescentes. Validación Del instrumento PHQ-9. *Rev. Médica Chile.* **146**, 479–486 (2018).
104. Rooney, S., McFadyen, D. A., Wood, D. L., Moffat, D. F. & Paul, P. L. Minimally important difference of the fatigue severity scale and modified fatigue impact scale in people with multiple sclerosis. *Mult Scler. Relat. Disord.* **35**, 158–163 (2019).
105. Nourbakhsh, B. et al. Longitudinal associations between brain structural changes and fatigue in early MS. *Mult Scler. Relat. Disord.* **5**, 29–33 (2016).
106. Rottoli, M., Gioia, S. L., Frigeni, B. & Barcella, V. Pathophysiology, assessment and management of multiple sclerosis fatigue: an update. *Expert Rev. Neurother.* **17**, 373–379 (2017).
107. Rao, S. M., Leo, G. J., Bernardin, L. & Unverzagt, F. Cognitive dysfunction in multiple sclerosis.: I. Frequency, patterns, and prediction. *Neurology* **41**, 685–691 (1991).
108. Smith & A. *SDMT: Test De Símbolos Y Dígitos: Manual* (TEA, 2002).
109. Ivanovic, D. et al. Brain structural parameters correlate with university selection test outcomes in Chilean high school graduates. *Sci. Rep.* **12**, 20562 (2022).
110. Glasser, M. F. et al. The minimal preprocessing pipelines for the human connectome project. *NeuroImage* **80**, 105–124 (2013).
111. Desikan, R. S. et al. An automated labeling system for subdividing the human cerebral cortex on MRI scans into gyral based regions of interest. *NeuroImage* **31**, 968–980 (2006).
112. Kucukboyaci, N. E. et al. Integration of multimodal MRI data via PCA to explain Language performance. *NeuroImage: Clin.* **5**, 197–207 (2014).
113. Liu, Y. & Tong, X. A. Tutorial on bayesian linear regression with compositional predictors using JAGS. *J. Behav. Data Sci.* **4**, 81–104 (2024).
114. Brink-Jensen, K. & Ekstrøm, C. T. Inference for feature selection using the Lasso with high-dimensional data. *ArXiv* <https://doi.org/10.48550/arxiv.1403.4296> (2014).
115. Tournier, J. D. et al. MRtrix3: A fast, flexible and open software framework for medical image processing and visualisation. *NeuroImage* **202**, 116137 (2019).
116. Ryali, S., Zhang, Y., Angeles, C., de los, Supekar, K. & Menon, V. Deep learning models reveal replicable, generalizable, and behaviorally relevant sex differences in human functional brain organization. *Proc. Natl. Acad. Sci.* **121**, e2310012121 (2024).
117. Dyken, P. C. V., Khan, A. R. & Palaniyappan, L. Imaging of the superficial white matter in health and disease. *Imaging Neurosci.* **2**, 1–35 (2024).

## Author contributions

AF-V, FA, RH-C, PG, CC, EC, and PB conceptualized the study. MV, BS, CM, MI-C, MPM-M, PC-P, MA-O, XS, CM, VM-R, PF-T, MD-D, JH, and FZ collected the data. AF-V, SN, PG, and PB analyzed the data. AF-V, SN, FA, PG, and PB wrote the main manuscripts and prepared the figures. All authors reviewed the manuscript.

## Funding

This work was supported by Agencia Nacional de Investigación y Desarrollo de Chile (ANID), Beca Doctorado Nacional 220711001, FONDECYT (1211227 and 1251073 to PB, AF-V), FONDEQUIP EQM150076, ANID-Basal Project FB0008 (AC3E) to PG.

## Declarations

## Competing interests

The authors declare no competing interests.

## Additional information

**Correspondence** and requests for materials should be addressed to A.F.-V., F.A. or P.B.

**Reprints and permissions information** is available at [www.nature.com/reprints](http://www.nature.com/reprints).

**Publisher's note** Springer Nature remains neutral with regard to jurisdictional claims in published maps and institutional affiliations.

**Open Access** This article is licensed under a Creative Commons Attribution-NonCommercial-NoDerivatives 4.0 International License, which permits any non-commercial use, sharing, distribution and reproduction in any medium or format, as long as you give appropriate credit to the original author(s) and the source, provide a link to the Creative Commons licence, and indicate if you modified the licensed material. You do not have permission under this licence to share adapted material derived from this article or parts of it. The images or other third party material in this article are included in the article's Creative Commons licence, unless indicated otherwise in a credit line to the material. If material is not included in the article's Creative Commons licence and your intended use is not permitted by statutory regulation or exceeds the permitted use, you will need to obtain permission directly from the copyright holder. To view a copy of this licence, visit <http://creativecommons.org/licenses/by-nc-nd/4.0/>.

© The Author(s) 2025